Accepted Article

Study of the Fractal Characteristics of the Cementation Index in Gas Shale

Hong-Qi Liu : *School of GeoScience and Technology, Southwest Petroleum of University, Chengdu, China,* 610500.

Email: LHQJP1@126.com

Shiqiong Liu : *School of GeoScience and Technology, Southwest Petroleum of University, Chengdu, China.*

Email : liushishi_hd67@outlook.com

Yangsha Sun : *School of GeoScience and Technology, Southwest Petroleum of University, Chengdu, China.*

sunyangsha1@126.com

Jie Tian : *School of GeoScience and Technology, Southwest Petroleum of University, Chengdu, China.*

TJ374050507@126.com

Lixi Liang : *Colledge of Petroleum Engineering, Southwest Petroleum of University.* Lianglixi@swpu.edu.cn

Sang Qin. : *School of GeoScience and Technology, Southwest Petroleum of University.* Sangq269@163.com

Xiangjun Liu : *School of GeoScience and Technology, Southwest Petroleum of University.*

Liuxiangjun@swpu.edu.cn

Abstract:

The description of pores and fracture structures is a consistently important issue and certainly a difficult problem, especially for shale or tight rocks. However, the exploitation of so-called unconventional energy, such as shale methane, tight-oil, has become more and more dependent on an understanding of the inner structure of these unconventional reservoirs. The inner structure of porous rocks is very difficult to describe quantitatively using normal mathematics, but fractal geometry, which is a powerful mathematical tool for describing irregularly shaped objects, can be applied to these rocks. To some degree, the cementation index and tortuosity can be used to describe the complexity of these structures. The cementation index can be acquired through electro-lithology experiments, but until now, tortuosity could not be quantitatively depicted. This research used

This article has been accepted for publication and undergone full peer review but has not been through the copyediting, typesetting, pagination and proofreading process, which may lead to differences between this version and the Version of Record. Please cite this article as doi: 10.1111/1755-6724.14302.

This article is protected by copyright. All rights reserved.

Accepted Article

the well-logging curves of a gas shale formation to reflect the characteristics of the rock formations and changes in the curves to indicate the changes of the rock matrix, the pores, the connections among the pores, the permeability, and the fluid type. The curves that are affected most by the rock lithology, such as the gamma ray, acoustic logging, and deep resistivity curves, can provide significant information about the micro- or nano-structure of the rocks. If the rock structures have fractal characteristics, the logging curves will also have fractal properties. Based on the definition of a fractal dimension and the Hausdorff dimension, this paper presents a new methodology for calculating fractal dimensions of logging curves. This paper also reveals the deep meaning of rock cementation index, *m*, through the Hausdorff dimension and provides a new equation to calculate this parameter through the resistivity and porosity of the formation. Although it represents a very important relationship between the saturation of hydrocarbon with pores and resistivity, the Archie formula was not available for shale and tight rock. The major reason for this was an incorrect understanding of the cementation index, and the calculation of the saturation used a single *m* value from bottom to top of the well. Unfortunately, this processing method is clearly wrong for the intensive heterogeneous material of shale and tight rock. This paper proposes a method to calculate *m* through well-logging curves based on a fractal geometry that can change with different lithology, so it would have more agreement with in situ situations than the traditional method.

Key words: **fractal geometry, nano-scale, well-logging curve, cementation index, tight rocks, gas shale**

I. Introduction

The novel concept of describing certain natural nonlinear, discrete, and rough objects with fractals was first introduced by Mandelbrot in 1967, and got more and more applied in various domains. (Mandelbrot, 1967, 1989; Feng, 2004; Freiberg, 2005; Lokenath, 2006; David, 2007; Naotaka, 2009). Fractal objects and processes have scale dependence, self-similarity, complexity, and infinite lengths or details. (Hu, 2006, Steinhurst, 2013, Naotaka, 2014)However, it is difficult to formally define the sufficient and necessary conditions for an object with fractal properties. Since the publication of an extremely important book authored by Mandelbrot (1982), there has been an ever-growing interest in the application of fractal geometry concepts to a variety of geological patterns and phenomena, and research has shown that the micro-structure of pores, the fractures of rocks, and even the rocks themselves have the self-similarity features of fractals (Hewett, 1986, Korhn, 1986, 1989, 1992; Ozhovan, 1993; Xie, 1994, 1996, Yu, 2005; Othman 2010; Peng, 2011; Sakhaee, 2016;). Fractal geometry theory has been applied to simulate the heterogeneity of the pores and fractures of rocks in different reservoirs, with great success (Mandelbrot, 1986, 1982, 1989). In some cases, variations in permeability with height at a well borehole were found to obey fractal statistics, and the correlations implicit in fractal geometries allowed researchers to interpolate between the known permeabilities at the borehole. Examples in open

This article is protected by copyright. All rights reserved.

Accepted Article

literature reporting the use of fractal geostatistics to describe naturally occurring fractures in reservoirs are less common (Xie, 1993, 1994, 1996; Donald, 1997).

Generally speaking, a fractal distribution requires that the number of objects larger than a specified size has a power-law dependence on a measurement scale. In fact, the empirical applicability of power-law statistics to geological phenomena was used long before the concept of fractals was created. Power-law distributions are certainly not the only statistical distributions that have been applied to geological phenomena. A comprehensive presentation of the applications of fractals was presented by Feder (1988). Vicsek (1992) provided an extensive treatment of fractals emphasizing growth phenomena. Kaye (1989, 1993) described a broad range of fractal problems, emphasizing those involving particulate matter. Korvin (1992) considered many fractal applications in earth science. Many geologists and geophysicists have applied fractal geometry methods and developed new techniques to quantify geological features that were difficult to analyze using only classical Euclidean geological techniques (Sammis et al., 1986; Turcotte, 1992; Korvin, 1992; Barton, 1995; Perfect, 1997; Perugini et al. 2002; Holtz et al., 2004)

When describing reservoirs, it is important to characterize the pore structures and fractures, but this task is extremely difficult in the early phases of an oilfield. Undoubtedly, understanding and characterizing the structure of porous media quantitatively is of fundamental importance to many industrial engineering fields, such as petroleum exploration, mining, metallurgy, and civil and hydraulic engineering (Boer, 2003; Chen and Song, 2002; Bansal et al., 2010). For example, in petroleum exploration, the pore structure of the rock affects the oil recovery, the remediation of non-aqueous phase liquid contaminated soil, and the heat and mass transport in the packed beds (Rigby and Gladden, 1996; Boadu, 2000). As complex geological materials, rocks have discontinuous, non-homogeneous, multi-phase composite structures. Many irregular pores occur on different scales, and these pores affect the physical, mechanical, and chemical properties of the rock materials (Othman et al., 2010; Peng et al., 2011; Zhao, 2016), such as the strength, elastic modulus, diffusion, permeability, conductivity, wave velocity, particle surface adsorption, and the capacity of the rock reservoir (Boadu, 2000; Sanyal et al., 2006; Giorgio et al., 2014). Some researchers proposed an approach that is characterized by a strict adherence to the pore size distribution of real materials (Yu, 2005; Xu, 2015). Zheng and others thought that the fractal dimension Dp can be determined with the porosity φ and the ratio rmin/rmax in porous media. Similarly, the tortuosity and length of capillaries also exhibit the fractal scaling law. (Zheng et al., 2013a, b; Xu et al., 2013a): Xu and Tian et al. predicated the relative permeability of rocks through fractal dimension, and they believed that the distribution of the capillaries satisfies the fractal characteristic, the probability density function can be determined (Xu et al., 2013a, 2013b, 2017; Tian, 2015;). Wang and Ge et al. analyzed the fractal properties of NMR images and its corresponding pore structures(Wang, 2012; Ge, 2015).

In the last few decades, especially in the recent ten years, unconventional hydrocarbon reservoirs such as tight-rock, shale gas, and gas hydrates have been more actively developed(Zou,2011; Ran, 2016; Zhai, 2018;

This article is protected by copyright. All rights reserved.

Accepted Article

Zhou, 2018; Bao, 2018; Chen, 2018; Lu, 2018; Zhao, 2018). Therefore, micro- and nano-scale pore structures have become more important in descriptions of tight rock or shale(Zhang, 2015a; Xu, 2015, 2017; Ju, 2018) The important properties of such structures are: (1) Different scaling behavior on different scales, (2) Inhomogeneity, and (3) Anisotropy. For the pore structure of shale, fractal geometry reveals a well-known series of "sponges" that illustrates the pore size distribution and morphology of the shale. An example of this is the Sierpinski carpet or its corresponding 3D model, known as the Menger sponge. The planar and 3-D Sierpinski carpets (i=4, 3) can be created by a finite iteration according to the power-law. The Sierpinski carpet is often used to simulate porous microstructures, especially for porous rocks. Fig. 1 shows SEM images of the shale at different magnifications, showing different sizes of pores or fractures that are very similar. Tectonic movement created fractures with different sizes, and their natural distribution is much like that of the Sierpinski carpet. This phenomenon is often encountered in rocks, especially in tight and shale rocks.

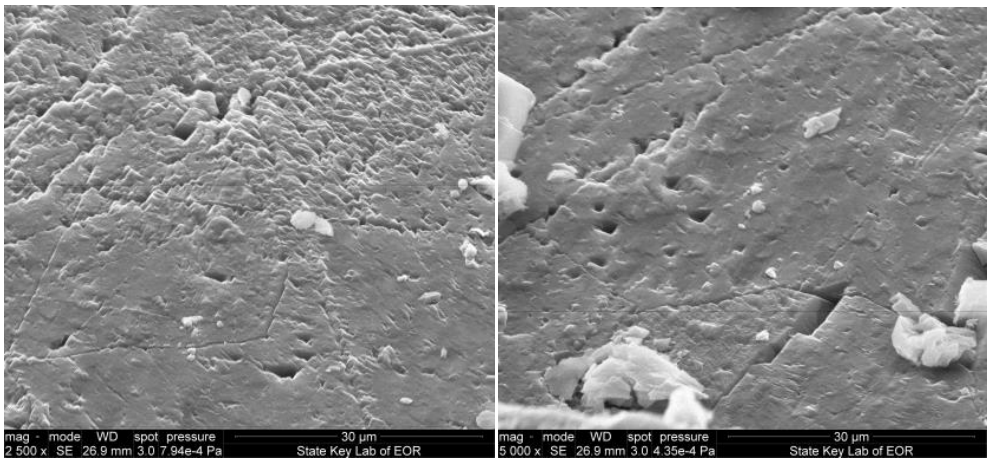

Fig. 1. Inner structure of the shale rock. Because of the tectonic movement, a lot of micro- or nano-scale pores and fractures with different sizes occurred, and their natural distribution is much like that of the Sierpinski carpet.

This article is protected by copyright. All rights reserved.

Accepted Article

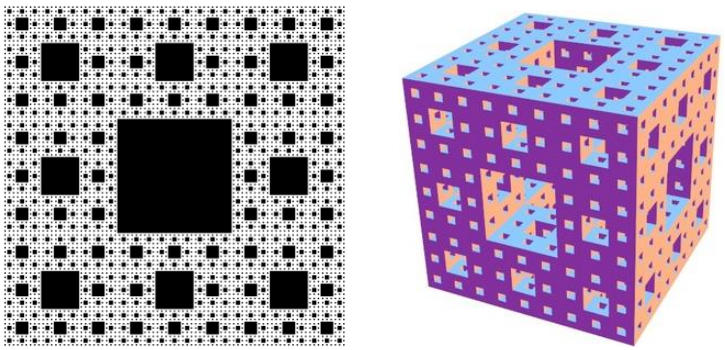

Fig. 2. Planar and 3-D Sierpinski carpet (i=4,3) that can be created by a finite iteration according to the power-law.

The SEM images in Fig. 3 show that the sizes of the pores and fractures range from the micrometer scale to the nanometer scale. It is very difficult to describe these pores or throat structures using classical geometry.

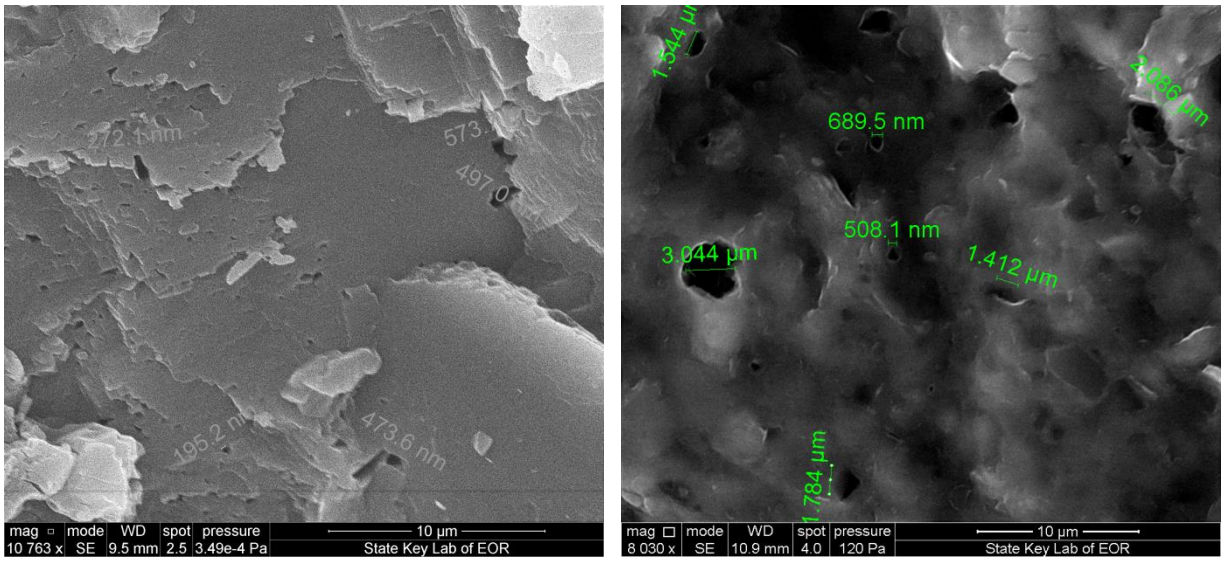

a) Kaolinite, ×10763, nanopores can be found b) Illinite, ×8030, micro- and nanopores can be found

This article is protected by copyright. All rights reserved.

Accepted Article

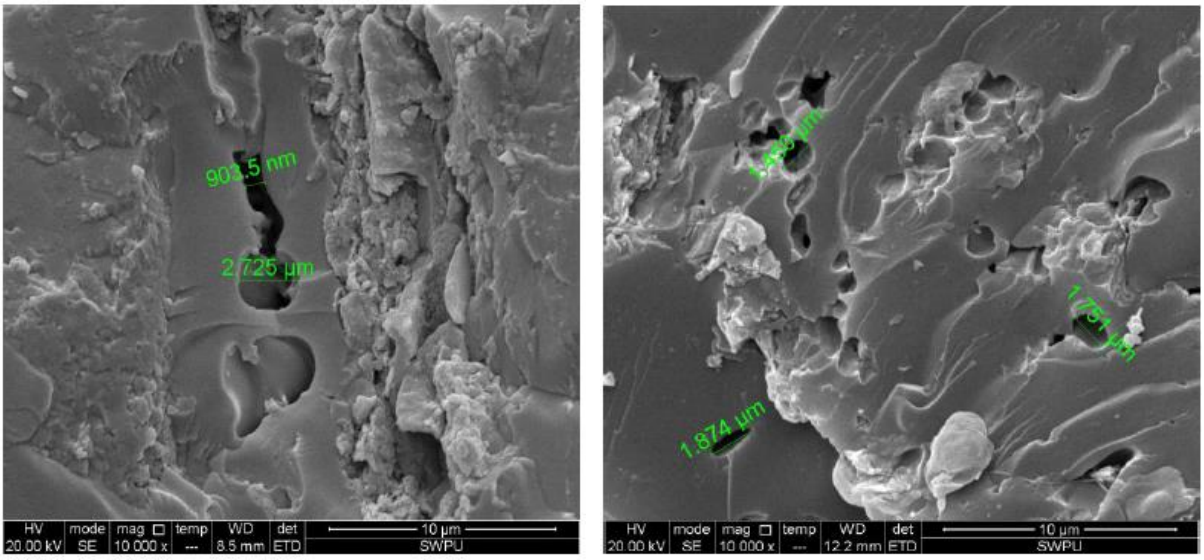

c) Illinite, ×10000, nano-throats and micropores d) Illinite, ×10000, micro-throats and micropores

Fig. 3. SEM images show that the pores, throats, and fractures have sizes that range from the micrometer to the nanometer range.

Both theoretical research and experimental studies show that sedimentary rocks have fractal pores, throats, and fractures. The real rocks are 3-D structures that are highly tortuous and often have fractal geometric forms. The geometric pore structures can be classified based on the crystallographic properties such as the shape, size, spatial distribution, and spatial and crystallographic orientation, combined with variations of the mineralogical and chemical composition, such as quartz, calcite, dolomite, and pyrite. The domains for these properties range from the nanometer-scale to the kilometer-scale. The large scale topography is created by tectonic processes, including faulting, folding, and flexure, and it is modified and destroyed by erosion and sedimentation. There is considerable empirical evidence that erosion is scale invariant and fractal. A river network is a classic example of a fractal tree. Topography often appears to be complex and chaotic, yet there is order in the complexity. Precise measurements of a wide spectrum of geological structures quantify different patterns of complexity on different scales. These methods of fractal geometry are the best and only choices for the pattern quantification of geological structures (Kaye, 1989, 1993), but it still difficult to use these methods to quantify the complexity of rock or formation environments.

Well-logging curves are derived from a variety of rock and formation properties, such as lithology, porosity, permeability, and pore structure. Therefore, all of these curves have fractal properties. This paper first presents a process for checking the fractal features of well-logging curves, and then shows how the fractal dimension Dw can be strictly derived according to mathematical definitions. Finally, the geological meaning of this fractal

This article is protected by copyright. All rights reserved.

Accepted Article

dimension is thoroughly described. We unexpectedly found that Dw had a relationship with the cementation index (m) of the formation, which is a very important parameter in the Archie equation (Archie, 1942). Our calculations of well-logging fractal properties further enlarged the geological meanings of m.

II. The Hausdorff Dimension and Fractal Properties of Logging Curves

1. Hausdorff dimension

Hausdorff and Hawkes expanded the classical dimension definition to depict functions that were continuous but not differentiable (Hausdorff, 1919; Hawkes, 1974), such as coast lines, chaos systems, and fractal forms (Haudm,1986; Donald etc. 1997).

We start our discussion with some basic definitions of set theory and the Hausdorff dimension. If U is a nonempty set, and if U $\in$ Rn, where R represents a real number set, the length or diameter of this set is defined as follows:

$$|U| = \sup\{|x-y|: x, y \in U\}. \tag{1}$$

The maximum spatial distance between any two different points is defined as the diameter of set U, and if {Ui} is an enumerable sequence, $X \subset \bigcup_{i=1}^{\infty} U_i$, $0 < U_i < \delta$, and $X \subset \bigcup_{i=1}^{\infty} U_i$, then {Ui} is a δ-overlap of set X. If $X \subset \bigcup_{i=1}^{\infty} U_i$, and D is non-negative ($\forall$ δ>0), then

$$H^D_{\delta(X)} = \inf\left\{\sum_{i=1}^{\infty} |U_i|^D\right\}. \tag{2}$$

If we use a smaller size of $\{U_i\}$ to decrease δ (δ→0), then

$$H^D_X = \lim_{\delta\to 0} H^D_{\delta(X)} = \lim_{\delta\to 0}\left\{\inf\left\{\sum_{i=1}^{\infty} |U_i|^D\right\}\right\} = \sup\sum_{i=1}^{\infty} |U_i|^D. \tag{3}$$

H^D_X increases with the decrease of δ, and H^D_X satisfies the definition of the measurement. If a limiting value of H^D_X exists for any subset $X \subset R^n$ (including 0 and ∞), then H^D_X is called a dimensional Hausdorff measure of subset *X* and it is represented by ***D*.**

For the sake of simplicity, Eq. 3 can be rewritten as

This article is protected by copyright. All rights reserved.

Accepted Article

$$D(X)=\lim_{\delta\to 0}\frac{\ln N(\delta)}{\ln(1/\delta)}=\lim_{\delta\to 0}\frac{\ln\left\{\sum_{i=2}^{k}\left|\frac{x_i-x_{i-1}}{\delta}\right|\right\}}{\ln(1/\delta)}. \quad (4)$$

2. Cross-point function of the well-logging curves

In set theory, well-logging curves are typically depth-time sequence data sets that contain the geophysical properties of the formation. Reservoirs are usually very heterogeneous, and many interbeds or thin layers are frequently encountered. The lithology and formation structures or the sedimentary environments can change significantly, and this change results in the complexity of the logging curves. Fig.4 illustrates a resistivity curve, labeled the deep resistivity, Rt, which represents the capability of the real formation's conduction. The curve's shape changes intensively, which indicates that the characteristics of the formation are greatly changed. A large change of the curve corresponds to an intensive change of the formation. Even if we use a relative large ruler to measure these changes, we can get a correspondence. Similarly, a small change reflects a small change of the formation. Even if a much smaller ruler is used, we can also find changes in the formation. Thus, the curve is much like the coastlines of an ocean, which have an infinite topology structure, and the curve can therefore be described through fractal geometry.

All of the logging data belongs to a real number set, Rn. If W represents a complete subset of the well-logging curve data, such as the gamma ray (GR), acoustic logging (AC), and deep resistivity (Rt) curves and so on, we can constitute real number subsets. For example, GR represents a real number set, the relationship of these three subsets is: $GR \subset W \subset Rn$.

As shown in the deep resistivity curve in Fig. 4, supposing that is Rt, the deep resistivity of the formation subset, and $Rt \subset W \subset Rn$, where Rn represents set of real numbers, then n is the dimension of real space, δ is the length of the side of square grid that is used to overlap the resistivity curve, and N (δ, i) is the cross-point function of two adjacent points. N (δ, i) is expressed as

$$N(Rt,\delta,i)=\mathrm{int}\left\{\frac{\left|Rt_i-Rt_{i-1}\right|}{\delta}\right\}, \quad (5)$$

where Rti is true resistivity of the ith point and int is a round function that returns an integer. Generally, the measure scale δ satisfies the condition δ<<|Rti-Rti-1|.

The number of cross points depends on two aspects. The larger the distance between two adjacent points is, the higher the value of N(r, i) is. The smaller the δ-grid scale is, the higher the value of the cross-point function is. For any zone of formation, assuming that there are k sampling points, the total number of cross points can be calculated by

This article is protected by copyright. All rights reserved.

Accepted Article

$$N(\delta)=\sum_{i=2}^{k}N_i=\sum_{i=2}^{k}\mathrm{int}\left\{\frac{\left|Rt_i-Rt_{i-1}\right|}{\delta}\right\}. \tag{6}$$

where k is the number of elements of this set, and N(δ) is a cross-point function of the well-logging curves. For other curves such as the AC curve used to calculate the porosity of a formation, we can get a similar cross-point function of N (δ).

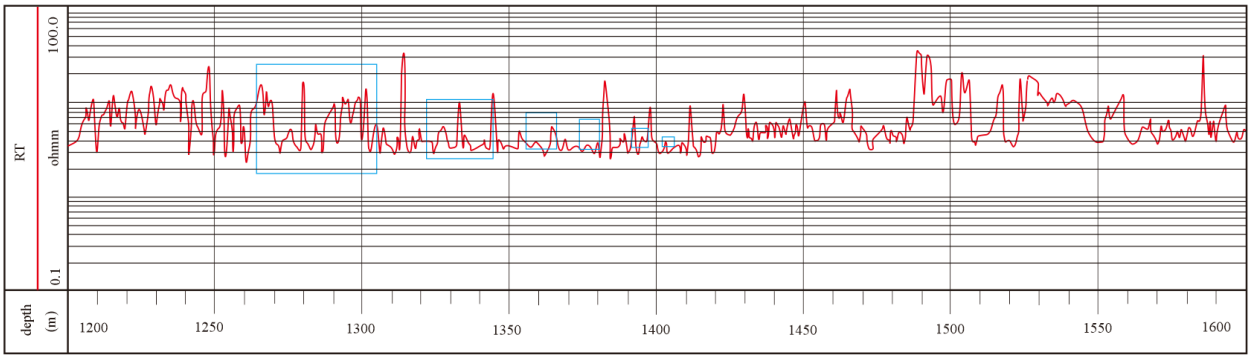

Fig. 4 Resistivity curve and Cross Function *N* (*δ*). This function is dependent on the change degree of the well-logging curve and the view-size of the square grid, i.e. the size of *δ*.

3. Formation cementation index

As we all know, the resistivity is a function of the porosity and saturation of water as well as its salinity. One of the classical equations for calculating saturation of hydrocarbons in formations is the Archie formula, it can be expressed as the following:

$$Sw=\sqrt[n]{\frac{abR_w}{\phi^m R_t}}, \tag{7}$$

where a and, b are generally taken as lithology coefficients, and usually, a=b=1. The parameter m, was named by Archie named it as the cementation index, which depicts the connectivity of different pores and throats, and n is the increscent coefficient of saturation. For several decades from Archie formula was published, thousands of papers have been presented to discuss the geological meanings and the value of m and n, especially the former. Many scholars presented their own modified models of this equation, including the Waxman-Smith model, the Dual water model, the Simandoux model and the Nigeria model, which are famous. Almost all of these models are focused on the conductivity of the formation water, and more importantly on the conductive path. Another

This article is protected by copyright. All rights reserved.

Accepted Article

significant definition was proposed, i.e. tortuosity, which will be discussed in detail later in this paper. In fact, many experts have noticed the complexity of the cementation index m, but ascertaining how to depict it is has been an eternal problem that disturbed them. Obviously, it cannot be defined by a linearized relation because of the complex topology of the structure of the pores and throats, especially their infinite inner and smaller micro- and nano-structures.

Fractal geometry has gained more and more attention since it was established by the famous mathematician Mandelbrot in 1975. It is a non-linear geometry that can be used to describe a natural phenomenon with statistical self-similarity. Through SEM, one can find this self-similarity phenomenon existence occasionally. Since *m* is related to the cementation of the pore and throat, and the pore and the throat have self-similarity, *m*, may consequently be expressed in fractal geometry form.

Eq. 7 can be rewritten as

$$R_t\phi^m = \frac{abR_w}{S_w^n}. \tag{8}$$

Any two adjacent points of the curve that were within a section of the reservoir have a thickness of 12.5cm or less. Therefore, generally speaking, less than 5 points cannot reflect a reservoir's properties. Therefore, the number of samples, *k*, is usually larger than 5.

If we have *k* points for a logging curve such as the Rt curve, then according to the Archie equation, the following formula can be deduced:

$$Rt_1\phi_1^m = Rt_2\phi_2^m = \bullet\bullet\bullet = Rt_{k-1}\phi_{k-1}^m = Rt_k\phi_k^m = \frac{abR_W}{S_W^n}. \tag{9}$$

For a certain layer of the geological profile in a well, the saturation of water, that is Sw, the resistivity of water, that is Rw is almost unchanged, and the coefficients of the rock *a* and *b* are also constant, so we get

$$Rt_1\phi_1^m = Rt_2\phi_2^m = \bullet\bullet\bullet = Rt_{k-1}\phi_{k-1}^m = Rt_k\phi_k^m = Rw. \tag{10}$$

To equate the two sides of this equation, we take the logarithm of each side and get

$$\ln Rt_1 + m\ln\phi_1 = \ln Rt_2 + m\ln\phi_2.$$

For any two different points, *i* and *j*, *m* can be derived:

This article is protected by copyright. All rights reserved.

Accepted Article

$$m_{ij} = -\frac{\ln Rt_i - \ln Rt_j}{\ln \phi_i - \ln \phi_j} \quad \left(i \neq j, and \quad \phi_i \neq \phi_j\right). \tag{11}$$

ln Rt_i is almost equal to ln Rt_j. If i and j are two adjacent points, the difference is almost 0. The same is true for ln φ_i and ln φ_j.

Eq. 11 has a limitation of 0/0, so it obeys l'Hôpital's rule or Bernoulli's rule. We can calculate these limitations one by one using a computer. If we calculate the values of m one by one according to the sequence based on Eq. 11, the equation can be further transformed into

$$m_i = -\frac{\ln Rt_i - \ln Rt_{i+1}}{\ln \phi_i - \ln \phi_{i+1}} = \frac{\left|\ln Rt_i - \ln Rt_{i+1}\right|}{\left|\ln \phi_i - \ln \phi_{i+1}\right|} \quad (\phi_i \neq \phi_{i+1} \quad and \quad i = 1, 2, ..., k-1). \tag{12}$$

The parameter m is usually determined by electro-lithological experiments with rock cores, but this is limited by the relatively high cost of cores extracted from formations and by the fact that core sampling is usually only done in specially selected zones. Therefore, an oilfield often has just one m for an entire area. If the reservoir is relative homogeneous, this is fine, but unfortunately, reservoirs are often very heterogeneous with different m values for different wells or even different m values for the same well with different formations. Because of this, Eq. 12 provides an effective method for calculating m without experiments.

4. Fractal properties of the cementation index *m*

If the denominator and numerator of Eq. 12 are both divided by the measure scale δ, we can get the Hausdorff fractal dimensions of R_t and φ. See Eqs. 5 and 6.

$$\frac{\left|\ln Rt_i - \ln Rt_{i+1}\right| / \delta}{\left|\ln \phi_i - \ln \phi_{i+1}\right| / \delta} = \frac{\sum_{i=1}^{k-1} \left|\ln Rt_i - \ln Rt_{i+1}\right| / \delta}{\sum_{i=1}^{k-1} \left|\ln \phi_i - \ln \phi_{i+1}\right| / \delta} \quad (\phi_i \neq \phi_{i+1} \quad and \quad i = 1, 2, ..., k-1). \tag{13}$$

And then we can get

$$\frac{\sum_{i=1}^{k-1} \left|\ln Rt_i - \ln Rt_{i+1}\right| / \delta}{\sum_{i=1}^{k-1} \left|\ln \phi_i - \ln \phi_{i+1}\right| / \delta} = \frac{\ln\left\{\sum_{i=1}^{k-1} \left|\ln Rt_i - \ln Rt_{i+1}\right| / \delta\right\} / \ln(1/\delta)}{\ln\left\{\sum_{i=1}^{k-1} \left|\ln \phi_i - \ln \phi_{i+1}\right| / \delta\right\} / \ln(1/\delta)} \quad (\phi_i \neq \phi_{i+1} \quad and \quad i = 1, 2, ..., k-1). \tag{14}$$

This article is protected by copyright. All rights reserved.

Accepted Article

If the saturation of the fluid in the formation is almost unchanged, and if the m_i (i=1,2,…, k-1) values are approximately equal to each other, based on the definition of the Hausdorff dimension, we can get

$$D_R = D(\ln Rt) = \lim_{\delta \to 0} \left\{ \frac{\ln \left\{ \sum_{i=1}^{k-1} \left| \frac{\ln Rt_i - \ln Rt_{i+1}}{\delta} \right| \right\}}{\ln(1/\delta)} \right\} \text{ and} \tag{15}$$

$$D_\phi = D(\ln \phi) = \lim_{\delta \to 0} \left\{ \frac{\ln \left\{ \sum_{i=1}^{k-1} \left| \frac{\ln \phi_i - \ln \phi_{i+1}}{\delta} \right| \right\}}{\ln(1/\delta)} \right\}. \tag{16}$$

Therefore, the Hausdorff dimensions for ln (R_t) and ln (φ) are

$$\delta^{1-D_R} = \sum_{i=1}^{k-1} \left| (\ln Rt_i - \ln Rt_{i+1}) \right| \text{ and} \tag{17}$$

$$\delta^{1-D_\phi} = \sum_{i=1}^{k-1} \left| (\ln \phi_i - \ln \phi_{i+1}) \right|. \tag{18}$$

Eqs. 14, 17, and 18 lead to

$$\mathrm{m} = \frac{\sum_{i=1}^{k-1} \left| (\ln Rt_i - \ln Rt_{i+1}) \right| / \delta}{\sum_{i=1}^{k-1} \left| (\ln \phi_i - \ln \phi_{i+1}) \right| / \delta} = \frac{\delta^{1-D_R}}{\delta^{1-D_\phi}}. \tag{19}$$

Therefore,

$$\mathrm{m} = \delta^{D_\phi - D_R}. \tag{20}$$

From the above discussion and calculations, based on the fractal properties of the pore structure of the rock, one can get a novel method for calculating the cementation index of a formation for a given zone of a reservoir. This method is much less expensive and more efficient than the normal electro-lithological experiments, but in addition to an effective calculation, this method also reveals the geological and geophysical meanings of *m*.

III. Fractal dimension of well-logging curves

In this research, we selected 6 samples of shale rock, and measured their organic porosity, inorganic porosity and total porosity respectively, and listed in Table 1. From the table, it was can be

This article is protected by copyright. All rights reserved.

Accepted Article

known the pore volume were very tiny, hence, their porosities were very low. And the SEM slips showed above illustrated the sizes of the pores were in micro or nano-scale, so if still use ordinary experiment to determine the value of m, the error was definitely large.

Table. 1 Porosity of shale cores

Sample No.	Organic Porosity /%	Inorganic Porosity /%	Total Porosity /%
1#	0.09-2.31	1.62-4.01	2.78-5.36
2#	0.10-1.46	1.28-3.22	2.02-4.28
3#	0.15-2.86	2.16-4.04	2.80-6.31
4#	0.06-1.35	2.23-4.37	3.02-5.26
5#	0.11-2.03	2.67-4.04	2.33-6.81
6#	0.16-2.44	2.27-4.83	2.05-6.93

The following section will clarify how to get this key parameter of ***m***.

Fig.5 and Table 2 show sample oilfield data. Using Eq. 20, ***m*** can be calculated for positions from the bottom to the top for a certain zone. Table 2 also shows values for the Hausdorff dimensions of resistivity and porosity curves with different measurement scales. This table shows that D_R and $D\varphi$ generally decrease with decreasing δ, but m stays equal to 2.120. The result is nearly in agreement with the measured value of m =2.173 that was derived from experiments. Supposing that R_w = 0.025 Ω·m, a=b=1, φ = 5.38%, n=2.0, and R_t = 89.65 Ω·m. If m = 2.173, then according to the Archie equation, S_w =39.997%, and if m =2.120, S_w =36.988%, then the relative error is only 7.45%.

Fig. 5 shows the three types of well-logging curves of an oilfield: The gamma ray reflected radioactivity of the formation (GR) curve, the resistivity of the true formation (Rt) curve, and the porosity of the formation (POR) curve. According to Eq. 18, we should use a variant view scale to create the Rt and POR curves. In this research, we used a rectangular grid and only the transverse side was changed. The vertical side, which represented the depth of the formation, was not changed, and was set to 0.1 m. The length of the transverse side was changed from 0.1 m to 10^{-4} m, so the grid size was 0.1 m to 10^{-4} m×0.1 m. For different curves, the transverse length of 0.1 m required different magnification amount (T_m). For example, the scale of the left side of the Rt curve was 0 Ω·m, and the scale of right said was 50 Ω·m. The transverse length of 0.1 m means that 0.1=(50-

This article is protected by copyright. All rights reserved.

Accepted Article

0)/T_m, so T_m =500 Ω·m. For the POR curve, T_m = (40-0)/0.1=400%, and for the GR curve, the T_m=(150-0)/0.1=1500 API. The view-scale is used like a magnifying lens to identify subtle and tiny changes in the curves. These changes reflect the micro- or nano-structure changes of the rocks.

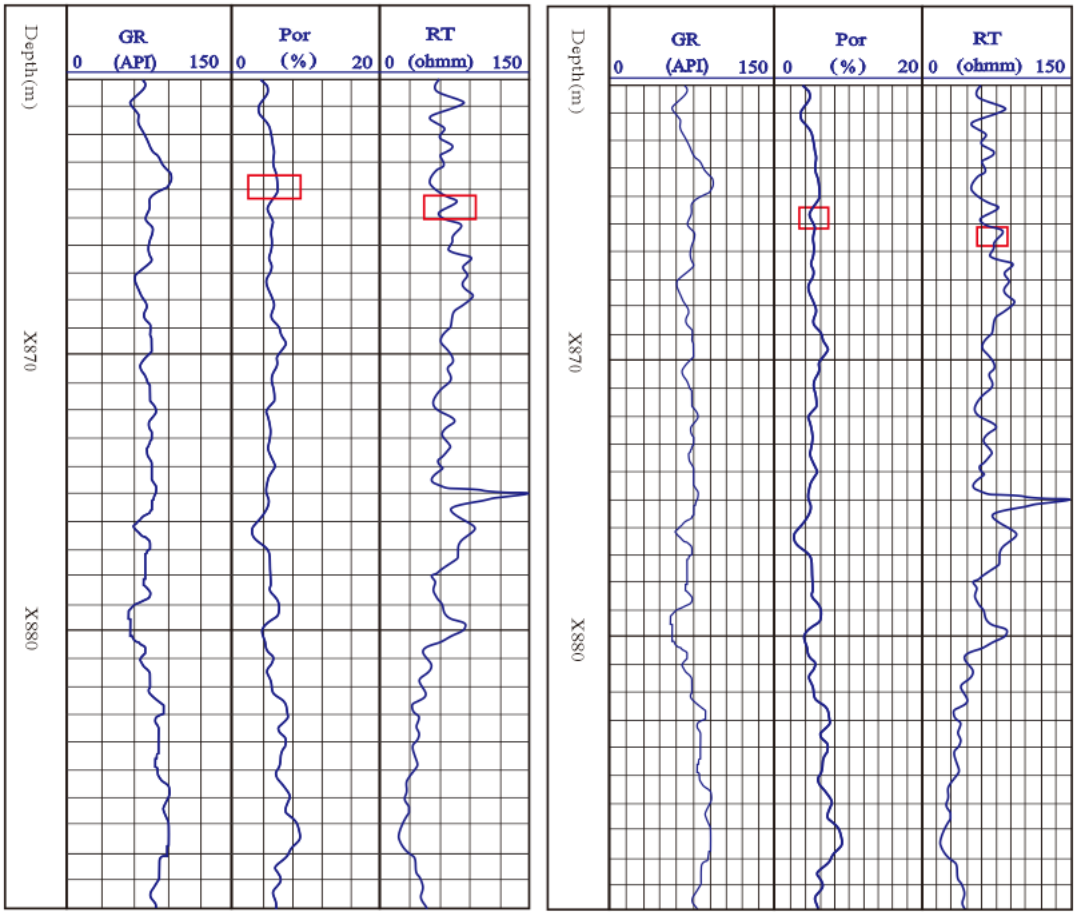

a) Grid size $\delta = 10^{-1}$ m×0.1 m b) Grid size $\delta = 10^{-2}$ m×0.1 m

This article is protected by copyright. All rights reserved.

Accepted Article

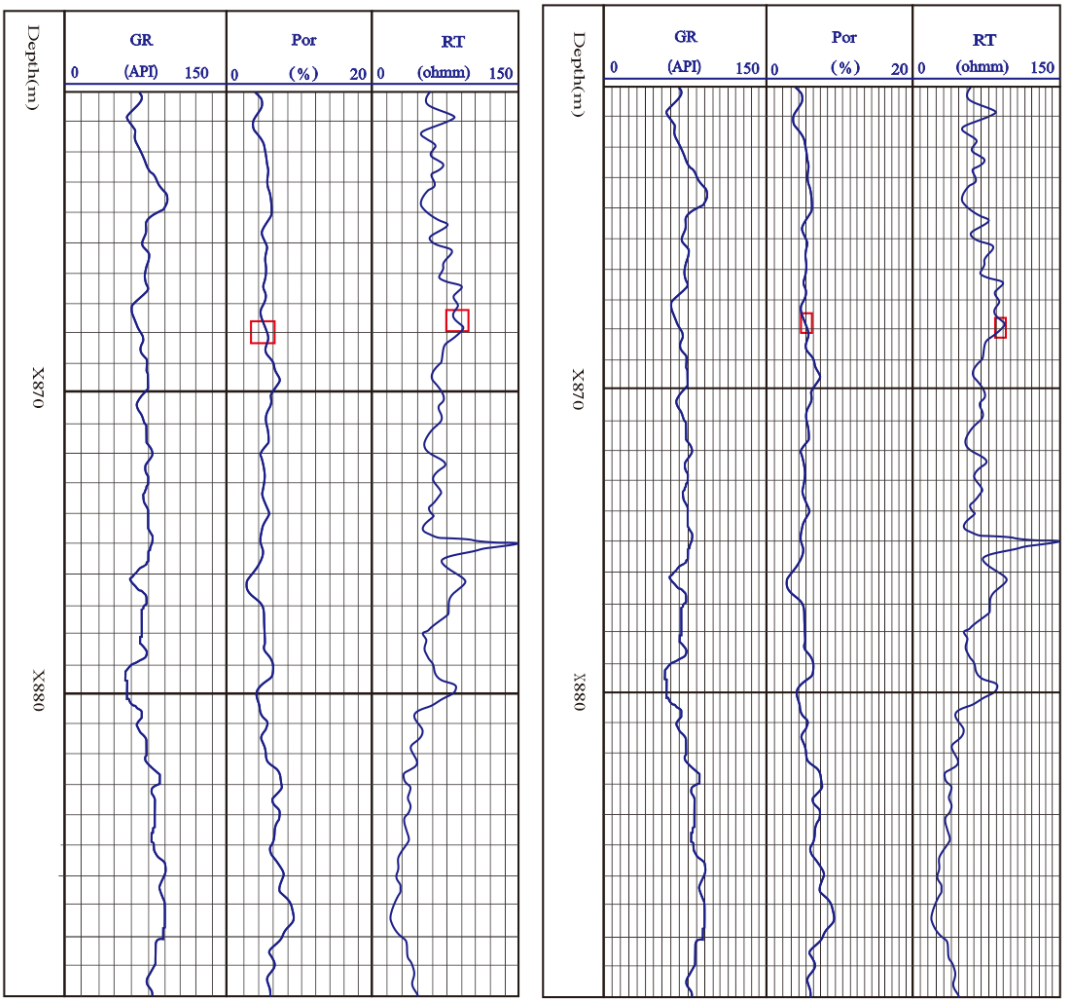

c) Grid size $\delta = 10^{-3}$ m×0.1 m

d) Grid size $\delta = 10^{-4}$ m×0.1 m

Fig. 5. GR, RT, and POR curves with different grid sizes.

Table 2. calculated *m* based on a fractal geometry grid size of $\delta = 10^{-1}$ m×0.1 m

Depth/m	GR/API	POR/%	Rt/Ω·m	$D\varphi$	D_R	m
X860	67.49	4.42	82.75	1.884	1.450	2.718
X861	58.07	4.29	76.25	1.029	0.980	1.119
X862	68.84	5.32	59.93	1.865	1.634	1.700
X863	84.47	5.49	63.22	1.621	1.236	2.426

This article is protected by copyright. All rights reserved.

Accepted Article

X864	84.93	5.80	55.31	1.317	1.256	1.150
X865	70.59	5.19	62.84	1.686	1.420	1.847
X866	63.42	5.24	86.94	1.943	1.875	1.170
X867	68.40	5.38	89.65	1.207	0.947	1.820
X868	72.24	6.00	76.93	1.304	1.217	1.223
X869	80.28	5.20	58.66	1.648	1.422	1.684
X870	75.15	5.48	64.00	1.827	1.691	1.368
X871	76.45	5.67	61.07	1.016	0.574	2.767
X872	62.59	4.26	86.03	1.639	1.377	1.828
X873	73.11	4.49	78.10	1.043	0.753	1.947
X874	69.62	5.53	52.02	1.292	0.972	2.092
X875	61.80	4.92	66.51	1.088	1.077	1.025
X876	56.09	4.07	80.65	0.902	0.619	1.920
X877	73.98	5.31	51.67	0.851	1.037	0.652
X878	83.10	7.34	41.83	1.849	1.763	1.218
X879	82.50	7.11	43.52	1.168	1.033	1.363
X880	81.69	6.08	35.17	0.972	0.902	1.175
X881	91.60	7.77	26.35	1.304	1.130	1.494
X882	91.61	8.71	22.22	1.187	1.003	1.528
X883	89.45	7.50	27.92	1.178	0.792	2.436

This article is protected by copyright. All rights reserved.

Accepted Article

X884	81.30	6.44	40.50	1.277	1.213	1.159
X885	81.70	5.70	46.63	1.014	0.709	2.019

IV. Geological and geophysical meanings of *m*

The cementation index, ***m***, is not just a value that describes the degree of intergranular cementation; it also reflects the subtle structure of the rocks and their evolution during the process of diagenesis. A rock's pore structure can be described by the fractal dimension $\boldsymbol{D_{\varphi}}$, and the rock's evolution is related to the distribution of water, oil, and gas, which can be depicted by the fractal dimension $\boldsymbol{D_R}$. Therefore, ***m*** is almost certainly a composite parameter, and what is most important is that ***m*** is associated with the content of the fluids and their spatial distribution. These issues affect the electrical current path. The more water there is in the rocks, the smaller of the resistivity is, but until now, it has not been clear how the electrons in direct or alternating currents penetrate the pores. The existence of oil and gas will impede the current path, but the question is how they will do that in porous rocks.

Supposing that the pore is completely saturated with water, then $\boldsymbol{S_w}$=100%. We can assume that the current takes the shortest, straight-line path with a total length represented by $\boldsymbol{L_w}$. For a straight line, the Hausdorff dimension of resistivity $\boldsymbol{D_R}$=1. With increasing hydrocarbon concentrations ($\boldsymbol{S_o}$), the path becomes tortuous and the length increases. The total length is represented by $\boldsymbol{L_h}$. Tortuosity, $\boldsymbol{T_C}$, can be used to describe the degree to which a current path is tortuous. It can be defined as

$$T_c = \frac{L_w}{L_h}. \tag{21}$$

T_c is always greater than or equal to 1.

V. Discussions

Fractal geometry provides methods for quantifying poorly defined geometries and patterns of extremely heterogeneous structures. This research discussed the fractal properties of the pore, throat, and fracture structures of shale rock. We used well-logging curves in our study because they reflect almost all of the properties of rocks and formations, which have fractal dimension characteristics that has been proved by many literatures (Donald et al., 1997; Chen et al., 2002; Boer et al., 2003). However, these literatures have pointed out that fractal geometry provides attractive and powerful tools for studying complex rock structures, and even others depicted the behavior of fluid in porous media(Hussain et al. 2012; Giorgio et al. 2013, 2014). Moreover some researchers have studied the

This article is protected by copyright. All rights reserved.

Accepted Article

fractal characteristics of shale and tight rocks (Lai et al., 2015; Tian et al., 2015; Sakhaee et al., 2016; Zhi et al., 2018). All of these literatures did not find the fractal property of cementation coefficient t of rocks, i.e. ***m***. Through rigorous mathematical proofs, this paper proved the vital parameter in Archie formula, ***m***, has fractal property, and can be calculated through well logging curves point by point. Equation (20) not only gives a more concise formula comparing with expensive and relative complicated experiment, it further reveals profound geological meanings of ***m***.

Eq. 20 shows that ***m*** not only reflects the degree of cementation, but most importantly, it discloses the micro- or nano-structures of the pores, throats, and fractures. Beyond helping to describe the spaces that contain fluids, determination of ***m*** also helps us to understand the evolution of the diagenesis and sedimentary environments.

VI. Conclusions

Our main objective in the present research was to study the fractal properties of the well logging curves and the rocks and the formations. We concluded as the following:

（1） The fractal dimensions reflect the dramatic changes of the logging curves, and the fractal dimensions generally decrease with decreasing of detection scale, $\boldsymbol{\delta}$.

（2） The Hausdorff dimensions of curves, R_t and $\boldsymbol{\varphi}$ were defined through a cross-point function, $N(\delta, i)$, making it possible to calculate the fractal dimensions D_φ and D_R.

（3） Based on the two parameters R_t and $\boldsymbol{\varphi}$, the cementation index ***m*** can be expressed in terms of the fractal dimensions.

（4） Because of the intensive heterogeneous of the shale and tight rock, the Archie formula was no longer available for these reservoirs. This paper proposed a method to calculate ***m*** using the well-logging curves based on fractal geometry, which can change with depth one by one, so it have more agreement with situations of in situ than the traditional method.

（5） More accurate ***m*** value ensures the engineers calculate $\boldsymbol{S_w}$ more precisely, and which has been validated by production data.

VI. Acknowledgments

The authors would like to thank graduate students Yu Deng, Jianqiao Yu and Dr. Bo Li for their work involving plotting and SEM analysis. This work was financially supported by The NSFC's (Natural Science Foundation of China, 2017ZX05001004-005) Research on The Technology of the Mutlilateral of Fluid Derivation During Sand Production. We also thank the editors and anonymous reviewers of this paper for their comments and valuable remarks.

This article is protected by copyright. All rights reserved.

Accepted Article

References

A. Sakhaee-Pour, Li, W.F., 2016. Fractal dimensions of shale. *Journal of Natural Gas Science and Engineering*. vol. 30 P578-582.

A.R. Bansal, G. Gabriel and V.P. Dimri, 2010. Power law distribution of susceptibility and density and its relation to seismic properties: An example from the German Continental Deep Drilling Program. *Journal of Applied Geophysics* Vol.72 No.2 123-128.

Anderson, A.N., McBratney, A.B., FitzPatrick, E.A., 1996. Soil mass, surface, and the spectral dimensions estimated from thin sections photographs. *Soil Sci. Soc. Am.* J. 60, 962-969.

Archie, G.E., 1942. The electrical resistivity log as an aid in determining some reservoir characteristics: Petroleum Transactions of the AIME, v. 146, p. 54-62.

B. B. Mandelbrot, A. Blumen, 1989. Fractal Geometry: What is it, and What Does it do [J]. *Proceedings of the Royal Society of London*. Serie. (1864)

Barnsley, M., 1988. Fractals Everywhere. *Academic Press.* Vol. 57 No.11 P1053 0002-9505

Boadu, F.K., 2000. Predicting the transport properties of fractured rocks from seismic information numerical experiments. *Journal of Applied Geophysics* 44, 103-113.

Boer, R., 2003. Reflections on the development of the theory of porous media. *Applied Mechanics Reviews* 56, 27-42.

C. G. Sammis, R. H. Osborne, J. L. Anderson, M. Banerdt, P. White, 1986. Self-similar cataclasis in the formation of fault gouge. *Pure and Applied Geophysics* Vol. 124 No.1-2 53-78.

Chen, Q., Song, Y.Q., 2002. What is the shape of pores in natural rocks. Journal of Chemical Physics 116, 8247-8250. *Math. Geol*. 20, 631, (1988).

Chen, F.W., Lu, S.F. and Ding, X., 2018. Pore Types and Quantitative Evaluation of Pore Volumes in the Longmaxi Formation Shale of Southeast Chongqing, China. *ACTA GEOLOGICA SINICA* (English Edition). Feb. Vol. 92 No. 1 pp.342–353.

David, C., Ben, H., 2007. Self-similarity and spectral asymptotics for the continuum random tree [J]. *Stochastic Processes and their Applications*. (5)730-754

De, J.F., 2005. The limited Rademacher functions and Bernoulli convolutions associated with Pisot numbers [J] . *Advances in Mathematics*. Vol. 195. P 24-101.

This article is protected by copyright. All rights reserved.

Accepted Article

Wang, D.H., Zhao Z., Yu Y et al., 2018. Exploration and research progress on ion-adsorption type REE deposit in South China, 1(3): 415-424. doi: 10.31035/cg2018022

Donald, L. Turcotte, 1997. Fractals and chaos in geology and geophysics, Cambridge University Press, Cambridge, U.K. Vol. 14. P1277.

F. Hussain, Y. Cinar, P. Bedrikovetsky , 2012. A Semi-Analytical Model for Two Phase Immiscible Flow in Porous Media Honouring Capillary Pressure [J]. *Transport in Porous Media*. Vol. 192 No.1 P187-212.

Zhai, G.Y., Wang, Y.F., Zhou, Z., Yu S.F., Chen X.L., Zhang Y.X., 2018. Exploration and research progress of shale gas in China. *China Geology*, 1, 257272. doi: 10.31035/cg2018024.

Ge, X.M., Fan, Y.R., Zhu, X.J., Chen, Y.G., Li, R.Z., 2015. Determination of nuclear magnetic resonance T2 Cutoff value based on multifractal theory-An application in sandstone with complex pore structure. *Geophysics* 80 (1), D11–D21.

Gimenez, D., Perfect E., Rawls W. J., Pachepsky Y, 1997. Fractal models for predicting soil hydraulic properties: a review. *Eng Geol*. 48(3–4): 161–83.

Giorgio, P., Ulrico S., 2013. A geometrical fractal model for the porosity and thermal conductivity of insulating concrete. *Construction and Building Materials*: 44:551-556.

Giorgio, P., Ulrico,S.,2014. Case studies on the influence of microstructure voids on thermal conductivity in fractal porous media. *Case Studies in Thermal Engineering*. 2:8-13.

Hansen, J.P., Skjeltorp, A.T., 1988. Fractal pore space and rock permeability implications. *Phys. Rev*. B 38, 2635-2638.

Haudm, R.D., 1986. On the Hausdorff dimension of graphs and random recursive objects in dimensions and entropies in chaotic systems (eds Gmayer). *Springer- Verlay, Berlin*, 28-33.

Hausdorff, F., 1919. Dimension and ausseres mass. *Math. Ann.* 79: 157-159.

Hawkes, J., 1974. Hausdorff measure, entropy and independences of small sets. *Proc. London Math. Soc*. 28: 700-724.

Wang, H., Liu ,Y., Song, Y.C., Zhao, Y.C., Zhao, J.F., Wang, D.Y., 2012. Fractal analysis and its impact factors on pore structure of artificial cores based on the images obtained using magnetic resonance imaging [J]. *Journal of Applied Geophysics*.Vol.86 P70-81.

Hewett, T.A., 1986. "SPE 15386 Fractal Geostatistics for reservoir hetero's." Soc. Of Pet. Eng. Richardson, TX.

Hu, J.X., Lau, K.S., Ngai, S.M., 2006. Laplace operators related to self-similar measures on R d[J] . *Journal of Functional Analysis*. Vol.239 No.2 P542-565.

Jin Lai, Guiwen Wang, 2015. Fractal analysis of tight gas sandstones using high-pressure mercury intrusion techniques [J] . *Journal of Natural Gas Science and Engineering*. Vol.24 P185-196 1875-5100.

This article is protected by copyright. All rights reserved.

Accepted Article

Jörn H. Kruhl, 2013. Fractal-geometry techniques in the quantification of complex rock structures: A special view on scaling regimes, inhomogeneity and anisotropy. *Journal of Structural Geology* 46 2-21

Katz, A.J., Thompson, A.H., 1985. Fractal sandstone pores: implications for conductivity and pore formation. Phys. Rev. Lett. 54, 1325-1328.

Kaye, B.H., 1984. Fractal description of fine particle systems. In: Beddow, K. (Ed.), *Particle Characterization in Technology*, vol. 1. CRC Press, Boca Raton. Chapt. 5.

Kaye, B.H., 1989. A Random Walk through Fractal Dimensions. *VCH Publishers, Weinheim*.421

Kaye, B.H., 1993. Chaos and Complexity. VCH Publishers, Weinheim.

Kaye, B.H., 1994. Fractal Geometry and the Mining Industry, a Review. In: Kruhl, J.H. (Ed.), *Fractals and Dynamic Systems in Geoscience*. Springer, Berlin/Heidelberg/New York, pp. 233e245. P233-245

Kaye, B.H., Clark, G.G., 1985. Fractal Dimension of Extraterrestrial Fine particles. Dept. Physics Laur*entian University*, Sudbury, Ontario, Canada. 16 p.

Korhn, C.E., Thompson, A.H., 1986, Fractal sandstone pores: automated measurement using, scanning-electron-microscope images, Phys. *Rev. B*, 33(9), 6311-6374.

Korvin, G., 1989. Fractured but not fractal: fragmentation of the Gulf of Suez basement. Pure and *Applied Geophysics* 131, 2890-305.

Korvin, G., 1992. Fractal Models in the Earth Sciences. *Elsevier, p*. 396.

Lokenath Debnath, 2006. A brief historical introduction to fractals and fractal geometry [J]. *International Journal of Mathematical Education in Science and Technology.* Vol.37 NO.1 P29-50 0020-739x.

Naotaka Kajino, 2014. Log-Periodic Asymptotic Expansion of the Spectral Partition Function for Self-Similar Sets [J] . *Communications in Mathematical Physics.* Vol.328 No.3 P1341-1370.

Naotaka Kajino, 2009. Spectral asymptotics for Laplacians on self-similar sets [J]. *Journal of Functional Analysis.* Vol.258 No.4 P1310-1360.

Neng-you Wu, Chang-ling Liu, Xi-luo Hao, 2018. Experimental simulations and methods for natural gas hydrate analysis in China. 1(1): 61-71. doi: 10.31035/cg2018008.

Netrusov, Yu., Safarov, Yu., 2005. Weyl asymptotic formula for the Laplacian on domains with rough boundaries. Commun. *Math. Phys.* 253, 481–509.

Othman, M.R., Helwani, Z., Martunus, 2010. Simulated fractal permeability for porous membranes. *Applied Mathematical Modelling* 34 (9), 2452-2464.

Ozhovan, M.I., Dmitriev, I.E., Batyukhnova, O.G., 1993. Fractal structure of pores in clay soil. At. Energ. 74 (3), 256-258.

Xu, P., BYu, .M., Qiao, X.W., Qiu, S.X., Jiang, Z.T., 2013. Radial permeability of fractured porous media by Monte Carlo simulations [J] . *International Journal of Heat and Mass Transfer.* (1)

Xu, P., Qiu, S.X., Yu, B.M., Jiang, Z.T., 2013. Prediction of relative permeability in unsaturated porous media with a fractal approach [J]. *International Journal of Heat and Mass Transfer*. Vol 64 P829-837.

This article is protected by copyright. All rights reserved.

Accepted Article

Peng, R., Yang, Y., Ju, Y., Mao, L., Yang, Y., 2011. Computation of fractal dimension of rock pores based on gray CT images. *Chinese Science Bulletin* 56 (31), 3346-3357.

Perugini, D., Speziali, A., Caricchi, L., Kueppers, U., 2011. Application of fractal fragmentation theory to natural pyroclastic deposits: insights into volcanic explosivity of the Valentano scoria cone (Italy). *Journal of Volcanology and Geothermal Research* 2002, 200-210.

Qian Zheng, Boming Yu, Yonggang Duan, Quantang Fang, 2013. A fractal model for gas slippage factor in porous media in the slip flow regime [J]. Chemical Engineering Science. Vol.87 P209-215 0009-2509.

Rigby SP.;Gladden LF, 1996. Nmr And Fractal Modelling Studies Of Transport In Porous. Chemical *Engineering Science* Vol.51 NO.10 2263-2272.

Sanyal, D., Ramachandrarao, P., Gupta, O.P., 2006. A fractal description of transport phenomena in dendritic porous network. *Chemical Engineering Science* 61(2), 307-315.

Shabro, Vahid, Kelly, Shaina, Torres-Verdín, Carlos, Sepehrnoori, Kamy, Revil, Andre, 2014. Pore-scale modeling of electrical resistivity and permeability in FIB-SEM images of organic mudrock. *Geophysics* 79 (5), D289-D299.

Bao, S.J., Zhai, G.Y., Zhou, Z., Yu, S.F., Chen, K., Wang, Y.F., Wang, H., Liu, Y.M., 2018. The evolution of the Huangling uplift and its control on the accumulation and preservation of shale gas, *China Geology*, 1, 346-353. doi: 10.31035/cg2018052.

Sondergeld, Carl H., Newsham, Kent Edward, Comisky, Joseph Thomas, Craig Rice, Morgan, Rai, Chandra Shekhar, 2010. Petrophysical considerations in evaluating and producing shale gas resources. *In: SPE Unconventional Gas Conference.*

Steinhurst, B.A.,Teplyaev, A., 2013. Existence of a meromorphic extension of spectral zeta functions on fractals. Lett. *Math. Phys.* 103, 1377–1388.

Tang, Xianglu, Jiang, Zhenxue, Li, Zhuo, et al.. 2015. The effect of the variation in material composition on the heterogeneous pore structure of high-maturity shale of the Silurian Longmaxi formation in the southeastern Sichuan Basin, China. *J. Nat. Gas Sci. Eng.* 23, 464-473.

Tsakiroglou, C.D., Payatakes, A.C., 2000. Characterization of the pore structure of reservoir rocks with the aid of serial sectioning analysis, mercury porosimetry and network simulation. *Advances in Water Resources* 23, 773-789.

Turcotte, D.L., 1997. Fractals and Chaos in Geology and Geophysics, second ed. Cambridge University Press, Cambridge. Vol. 36 P 131-132.

Uta Freiberg, 2005. Spectral Asymptotics of Generalized Measure Geometric Laplacians on Cantor Like Sets [J]. *Forum Mathematicum.* Vol.17 NO.1 P87-104 0933-7741.

Vicsek, Tamas, 1992. Fractal Growth Phenomena, 2nd edition.World Scientific Publishing Co. Pvt. Ltd.

Wildenschild, Dorthe, Sheppard, Adrian P., 2013. X-ray imaging and analysis techniques for quantifying pore-scale structure and processes in subsurface porous medium systems. *Adv. Water Resour.* 51, 217-246.

This article is protected by copyright. All rights reserved.

Accepted Article

Tian, X.F., Cheng, L.S., Yan, Y.Q., Liu, H.G., Zhao, W.Q., Guo, Q., 2015. An improved solution to estimate relative permeability in tight oil reservoirs [J]. *Journal of Petroleum Exploration and Production* T. Vol.5 No.3 P305-314.

Chen, X.H., Luo, S.Y., Liu, A., Li, H., 2018. The oldest shale gas reservoirs in southern margin of Huangling uplift, Yichang, Hubei, China, *China Geology*, 1, 158-159.

Tan, X.H., Liu J.Y., Li X.P., et al, 2015. A simulation method for permeability of porous media based on multiple fractal model. *International Journal of Engineering Science* 95. 76-84.

Duan, X.Y., Li, Y.X., Li, X.G., et al. Historical records and the sources of polycyclic aromatic hydrocarbons in the East China Sea. 2018, 1(4): 505-511.

Xie H, 1993. "fractals in rock mechanics." Geomechanics research Series. Kwasniewski ed. A. A. Balkema. Rotterdam.

Xie, H. & Pariseau, W.G., 1994. Fractal estimation of joint roughness coefficients. *Science in China* (Seires B), 37(12),1516-1524.

Xie, H., Wang, J.A., Kawasniewski, M.A., 1996. Fractal effect of surface roughness on the mechanical behavior of rock joints, chaos, *solitons & Fractals*, 7(10), 1-32.

Zhao, X.M., Song, F.Y., Deng, J., et al, 2018. New indications of gas hydrate in the northeastern China permafrost zone. *China Geology*, 1, 308-309.

Xu, P., 2015. A discussion on fractal models for transport physics of porous media. *Fractals* 23 (03), 1530001.

Xu, P., Qiu, S.X., Cai, J.C., Li, C.H., Liu, H.C., 2017. A novel analytical solution for gas diffusion in multi-scale fuel cell porous media. *J. Power Sources* 362, 73–79.

Xu, P., Qiu, S.X., Yu, B.M., Jiang, Z.T., 2013a. Prediction of relative permeability in unsaturated porous media with a fractal approach. Int. J. Heat. *Mass Transf.* 64, 829–837.

Xu, P., Yu, B.M., Qiao, X.W., Qiu, S.X., Jiang, Z.T., 2013b. Radial permeability of fractured porous media by Monte Carlo simulations. Int. J. Heat. *Mass Transf*. 57 (1), 369–374.

Li, Y.C., Zhang, K.X., He W.H., et al., 2018. Division of tectonic–strata superregions in China. 1(2): 236-256. doi: 10.31035/2018028

Ju, Y.W., Cheng H., Sun, Y., et al., 2018. Nanogeology in China: A review. *China Geology*. 1(2): 286-303. doi: 10.31035/2018020

Yu, B.M., 2005. Fractal character for tortuous stream tubes in porous media. *Chin. Phys. Lett*. 22 (1), 158–160.

Wan, Y.S., Liu, S.J., Xie, H.Q., et al., 2018. Formation and evolution of the Archean continental crust of China: A review. *China Geology*. 1(1): 109-136. doi: 10.31035/2018011

Zhang, L.G., Li, D.L., Lu, D.T., Zhang, T., 2015b. A new formulation of apparent permeability for gas transport in shale. J. *Nat. Gas Sci. Eng.* 23, 221-226.

This article is protected by copyright. All rights reserved.

Accepted Article

Zhang, Q., Su, Y.l., Wang, W.D., Sheng, G.L, 2015a. A new semi-analytical model for simulating the effectively stimulated volume of fractured wells in tight reservoirs. J. Nat. *Gas Sci. Eng.* Vol.27 P1834-1845 .

Zhao J.H., Jin Z.J., Jin Z.K., et al, 2016. Physical mechanism of organic matter-mineral interaction in Longmaxi Shale, Sichuan Basin, China. *Acta Geologica Sinica* (English Edition), 90(5): 1923–1924.

Lu, Z.Q., Zhai, G.Y., Zhu, Y.H., et al, 2018. New discovery of the permafrost gas hydrate accumulation in Qilian Mountain, China, *China Geology*, 1, 306-307.

Zhou Z., Bao SJ , Chen XL,et al, 2018. A discovery of Silurian tight shale gas in Jianshi, Hubei, China, *China Geology*, 1, 160-161.

Zou, C.N., Zhu, R.K., Bai B., et al, 2011. First discovery of nano-pore throat in oil and gas reservoir in China and its scientific value. *Acta Petrologica Sinica*, 27(6): 1857–1864(in Chinese with English abstract).

This article is protected by copyright. All rights reserved.